Long-period Milankovitch cycles from the Late Triassic and Early Jurassic of eastern North America and their implications for the calibration of the Early Mesozoic time-scale and the long-term behaviour of the planets

By Paul E. Olsen[1] and Dennis V. Kent[2]

[1] Lamont-Doherty Earth Observatory of Columbia University, Rt 9W, Palisades,
NY 10964, USA (polsen@ldeo.columbia.edu)
[2] Department of Geological Sciences, Rutgers University, Piscataway, NJ 08854,
USA and Lamont-Doherty Earth Observatory of Columbia University, Rt 9W,
Palisades, NY 10964, USA (dvk@ldeo.columbia.edu)

During the Late Triassic and Early Jurassic, the Newark rift basin of the northeastern US accumulated in excess of 5 km of continental, mostly lacustrine, strata that show a profound cyclicity caused by the astronomical forcing of tropical climate. The Newark record is known virtually in its entirety as a result of scientific and other coring and provides what is arguably one of the longest records of climate cyclicity available. Two proxies of water depth, and hence climate, in this record are a classification of sedimentary structures (depth ranks) and sediment colour. The depth rank and colour depth series display a full range of climatic precession related cycles. Here, we tune the depth rank and colour records to the 404 ka astronomical cycle and use this tuned record to explore the existence and origin of very long-period climate. We find highly significant periods of climatic precession modulation at periods of *ca.* 1.75 Ma, 1 Ma and 700 ka in not only the depth rank and colour records, but also in the sedimentation rate curve derived from the tuning process. We then use the colour and depth rank time-series to construct an astronomically tuned time-scale for the Late Triassic. While the Newark higher-frequency eccentricity cycles that modulate precession are indistinguishable from today, the 1.75 Ma cycle is significantly different from predictions based on the present day fundamental frequencies of the planets (i.e. Ma) and provides the first geological evidence of the chaotic behaviour of the inner planets, otherwise known only from numerical calculations.

Keywords: climate; Milankovitch; chaos; Triassic; cyclicity

1. Introduction

Continental rift basins are unique repositories for long-term palaeoclimate records. First, they are often dominated by lacustrine strata that are sensitive to climate change. Second, they tend to record comparatively local climate changes, as opposed to integrated global effects, as in the oceans. Third, they often have very high accumulation rates, which enhances the temporal resolution of their sedimentary records. Fourth, because rifts tend to be closed basins, deposition is unusually continuous.

Finally, rifts tend to subside for very long periods of time and hence their records often span tens of millions of years. One of the largest rift systems known formed during the Early Mesozoic initial fragmentation of Pangea, and one of the largest individual rifts in this system, the Newark Basin of New York, New Jersey and Pennsylvania (eastern US), has recently been cored almost in its entirety (Olsen & Kent 1990). This continuously cored sequence is comprised mostly of cyclical lacustrine strata displaying a full spectrum of precession-related orbitally forced cycles. It provides not only the longest record of continuous orbital forcing available (*ca.* 26 Ma), but also the only truly long record of tropical orbital forcing in a continental environment. The basic lithology and depositional environments (Olsen *et al.* 1996*a*), palaeomagnetic stratigraphy (Kent *et al.* 1995), Milankovitch cyclicity (Olsen & Kent 1996), and borehole geophysics and cyclicity (Reynolds 1993; Goldberg *et al.* 1994) have already been described. In addition, we have developed an astronomically tuned time-scale for the Late Triassic and earliest Jurassic based on these cores (Kent & Olsen 1999*a, b*).

In this paper we take advantage of the great length of this orbitally controlled lacustrine record to examine the long-period (*ca.* 400 ka to 4 Ma) orbitally forced cycles. We then use this record to derive a high-resolution time-scale of the Late Triassic and Early Jurassic that does not rely on the subjective identification of cycles (although they are easily observed). In addition, the fine structure of the Fourier spectra of Newark Basin records, tuned to the 404 ka cycle, allows calculation of a range for the fundamental frequencies of Mars, Earth and Mercury, and comparisons with predictions of the chaotic behaviour of the Solar System (e.g. Laskar 1990).

(*a*) *Geological and environmental background*

During the Triassic and Early Jurassic periods the Newark Basin developed as one of the largest of many rift basins on the extending crust between the North American and African plates (Van Houten 1977) (figure 1). Structurally, it is a half graben with major boundary faults on the northwest side of the basin towards which the strata dip. Presently, the Newark Basin is 180 km long and 60 km across and contains at least 5 km of seismically imaged section (Manspeizer 1988; Reynolds 1993). However, because several kilometres of basin section have been lost during post-rift erosion over the entire basin (Steckler *et al.* 1993; Malinconico 1997), it was originally considerably larger. The Newark Basin is connected to the Gettysburg Basin, and was formerly connected to the Culpeper Basin to the southwest. This basin complex was as large in area as the Lake Tanganyika or Baikal Rifts are today (Olsen 1997).

Rift strata of the Newark Basin are divided into nine lithologically recognized formations. The stratigraphically lowest of these is the red and grey, relatively coarse-grained fluvial and lacustrine Stockton Formation of Carnian age (early Late Triassic). This is followed by a very thick section of profoundly cyclic lacustrine strata of the mostly grey and black Lockatong Formation of late Carnian age and the mostly red Passaic Formation of Carnian, Norian, Rhaetian (later Triassic), and earliest Jurassic age. Hettangian age (Early Jurassic), mostly red, cyclical lacustrine strata interbedded with three basaltic lava flow formations constitute the youngest strata of the basin (i.e. Orange Mt Basalt, Feltville Formation, Preakness Basalt, Towaco Formation, Hook Mt Basalt and Boonton Formation).
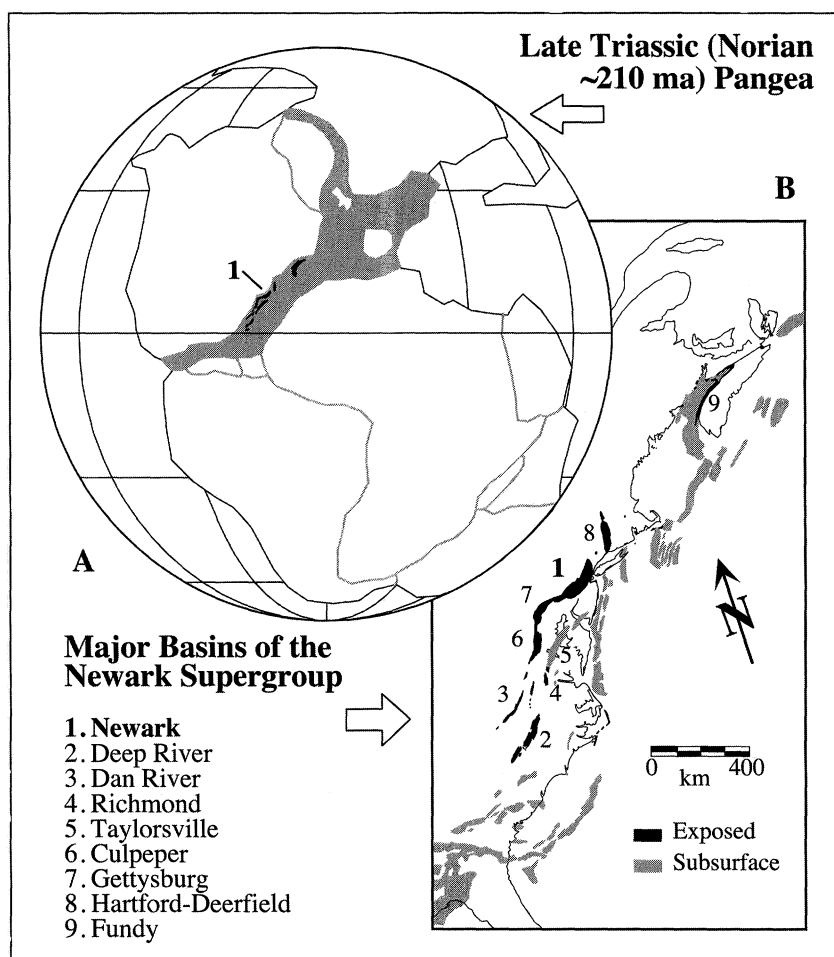
Figure 1. Pangea and the Newark rift basins (A), showing the position of the Newark rift basin (1) about midway through the Newark core record. Newark-type rift basins (B) in Eastern North America in present geography. Modified from Olsen *et al.* (1996*a*).

The conceptual justification for the US National Science Foundation-funded Newark Basin Coring Project (NBCP) was a series of outcrop studies that documented a large-scale lithological cyclicity with great lateral extent (McLaughlin 1946), orbital forcing in the *ca.* 20, *ca.* 100 and *ca.* 400 ka range (Van Houten 1969), and a recoverable, laterally correlatable palaeomagnetic stratigraphy (Witte *et al.* 1991). Together, these and other studies, only a few of which are mentioned here (see Olsen (1997) for summary), indicated that the Newark Basin section should contain a very detailed and very long continuous record of continental tropical orbital forcing, recoverable by continuous coring.

The NBCP recovered *ca.* 7 km of core at a total of seven stratigraphically contiguous sites spanning the Feltville through Stockton formations. With *ca.* 30% stratigraphic redundancy these cores produce a 4660 m thick composite section (figure 2). The Army Corps of Engineers (Fedosh & Smoot 1988) cored *ca.* 10 km of the Upper Passaic and virtually all of the rest of the Early Jurassic age section (Olsen *et al.*
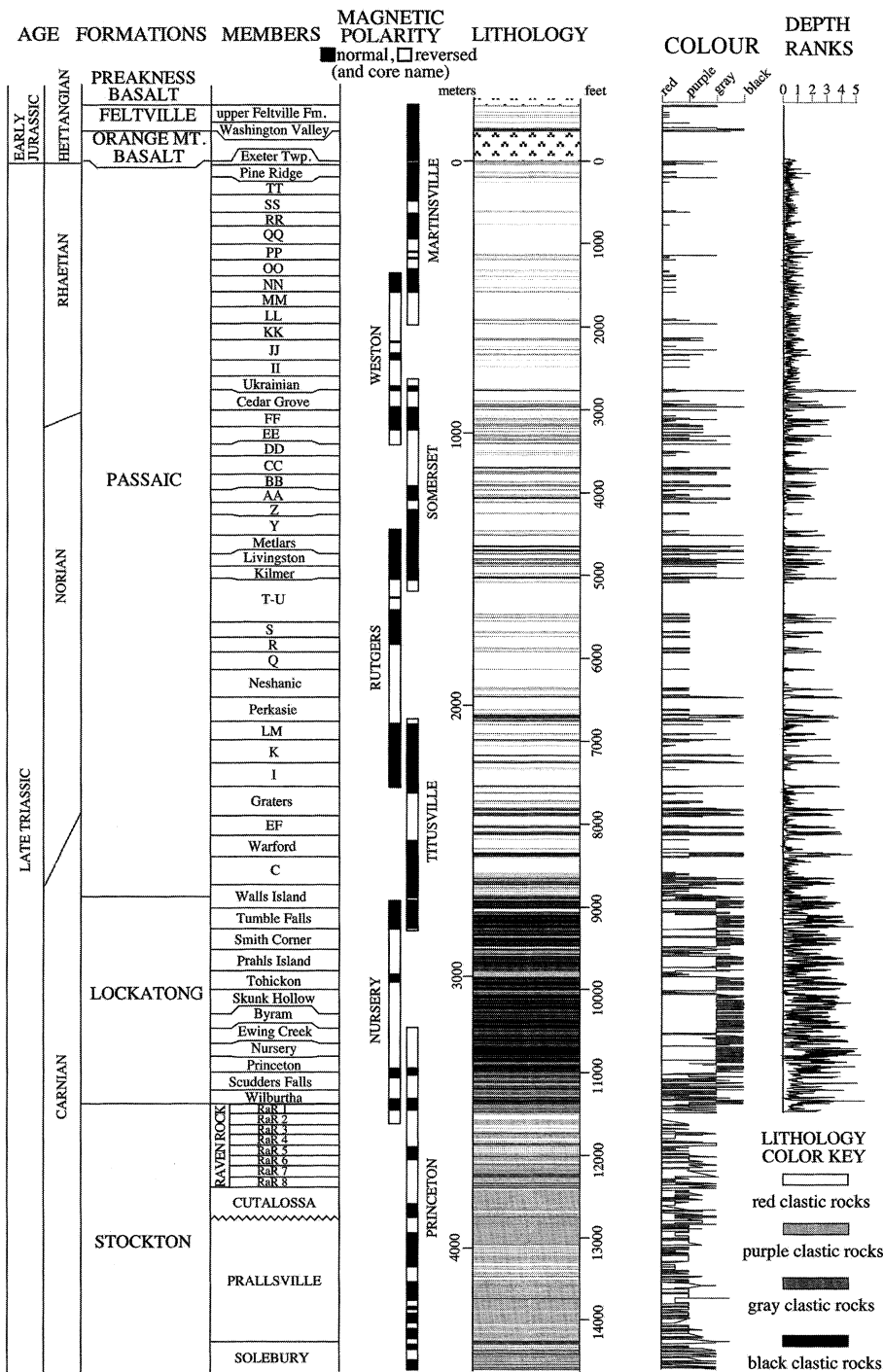
Figure 2. Newark Basin section in core depth showing original (untuned) colour and depth rank records. Zigzag line between Cutalossa members and Prallsville represents possible minor unconformity. Modified from Olsen & Kent (1996).
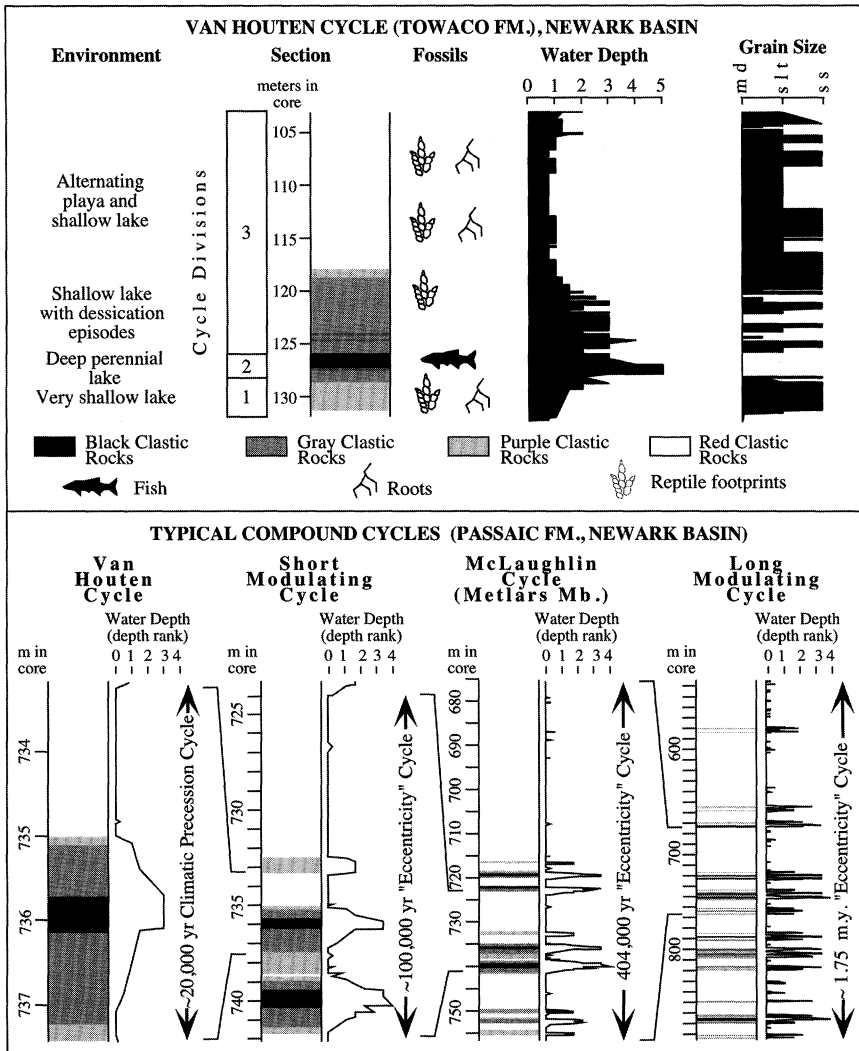
Figure 3. Typical Van Houten cycle and modulating (compound) cycles of the
Newark Basin cores (modified from Olsen (1997)).

1996*b*), thereby adding more than 1 km of additional stratigraphically continuous
section.

The basic lithological sequence displaying the climate cyclicity consists of a lake-
level sequence termed the Van Houten cycle (figure 3), named after its discoverer (Van
Houten 1969; Olsen 1986). Variations, largely in sedimentary structures and other
aspects of lithology, including colour, show that deposition of a single cycle occurred
during the expansion and contraction of a very large lake. Sequences deposited in
what were the deepest lakes have black microlaminated mudstones containing artic-
ulated fish and reptiles in strata deposited during high stands. Over- and under-
lying lake rise and fall deposits of such cycles are often grey or grey and red with
reptile footprints, zones of desiccation cracks and root zones. Van Houten cycles
deposited in what were the shallowest lakes have laminated red or purple mud-
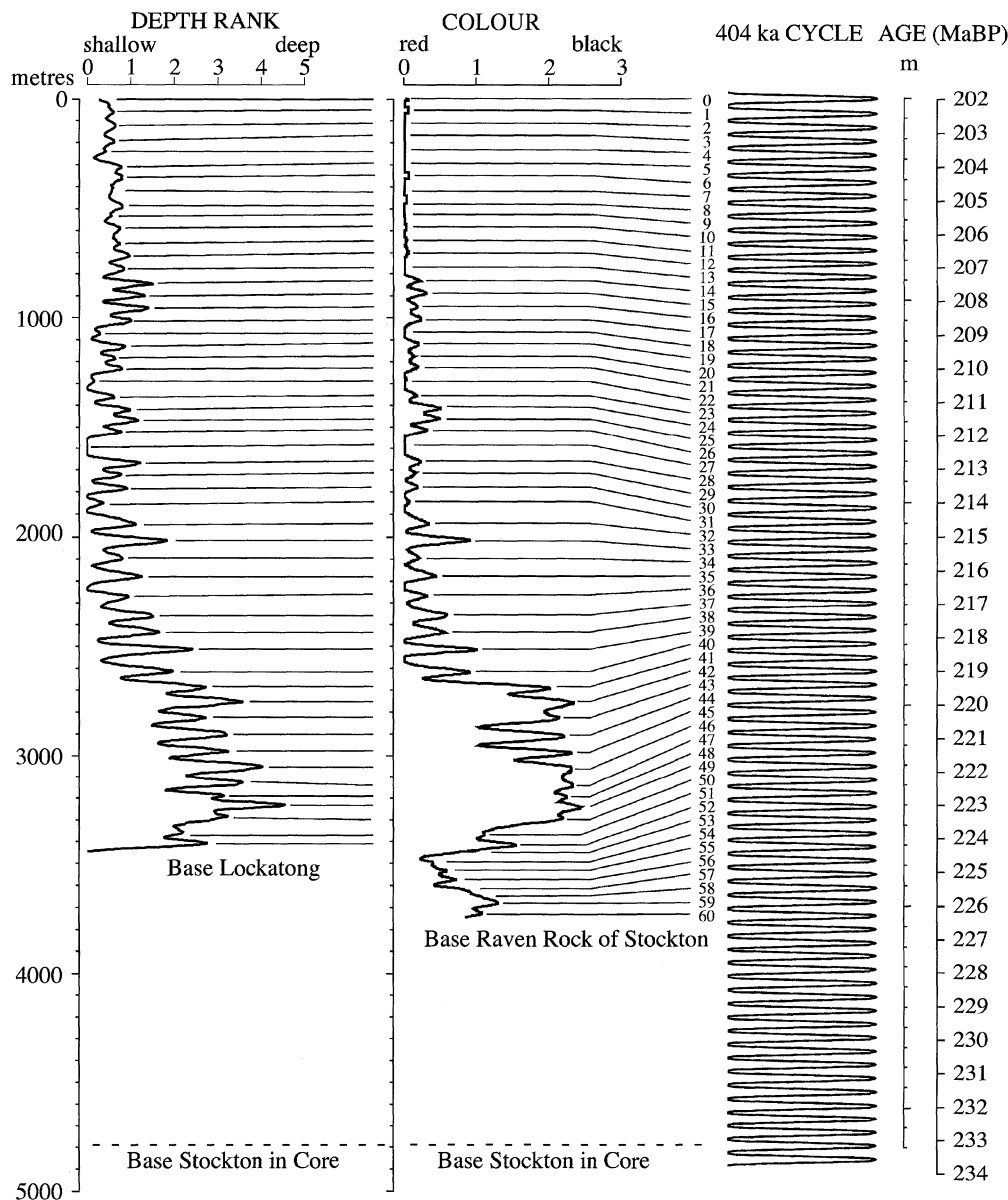
Figure 4. Smoothed depth rank and colour depth series and reference series composed of cycles with a period of 65.55 m (404 ka). Cores are shown at their original depth scale but the Martinsville and ACE cores are truncated upward at the base of the Orange Mountain Basalt (0 in the depth scale). Cycle numbers begin at 0 within the Jurassic section (Boonton Formation) for notation purposes here; but note that lithostratigraphic members were named and lettered upward from the base of the Lockatong (McLaughlin 1946; Olsen *et al.* 1996a).

stones or ripple-cross-laminated siltstones deposited during their high stands and massive mud-cracked red mudstones deposited during their transgressive and regressive deposits. The variations in sedimentary structures have been described in detail by Smoot & Olsen (1994). In broadest terms, when the lakes were at their deep-

Passaic Fm. |Lockatong Fm.| Stockton Fm.

Age (MaBP)

Core Composite Depth Scale (m)

Figure 5. Age versus depth relationship for the Newark Basin cores. Circles represent the peaks of the depth series in colour and the time-series of the 404 ka series (figure 4). Black circles are those for the fine-grained portion of the section with well-developed high-frequency Milankovich cycles (i.e. (100 ka and *ca.* 20 ka cycles), and white circles are peaks of McLaughlin-type cycles in the Stockton Formation represented primarily by sandstone. Boxes represent the thickness and time covered by individual cores as follows (from lower left to upper right): Martinsvil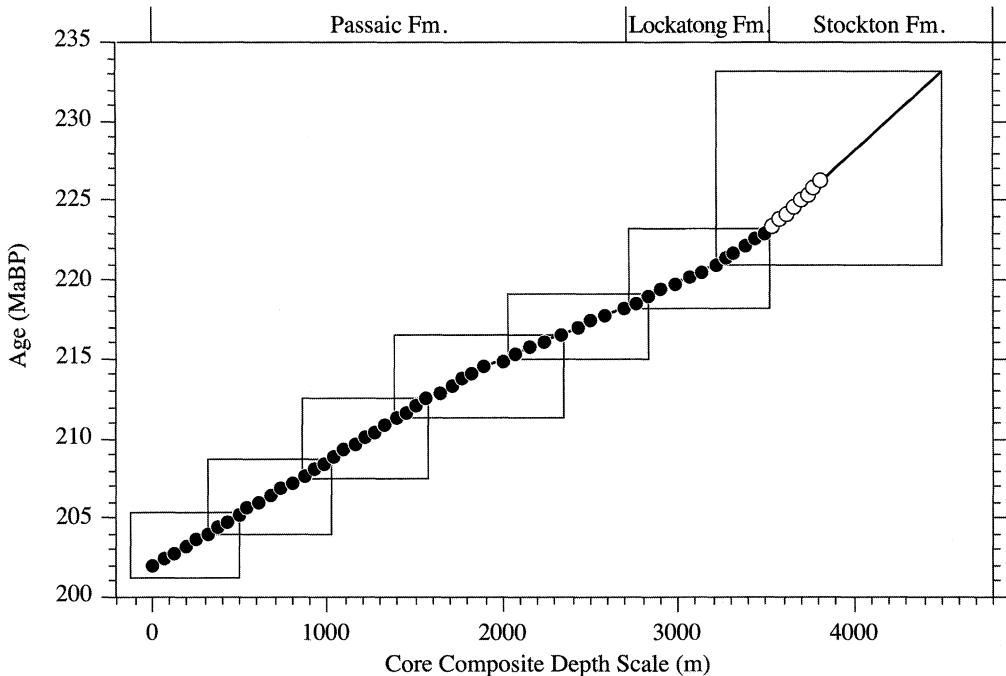le no. 1; Weston no. 1 and 2; Somerset nos 1 and 2; Rutgers nos 1 and 2; Titusville nos 1 and 2; Nursery no. 1; Princeton nos 1 and 2. Note that the long straight line segments correspond to the major sedimentation rate changes seen in figure 7.

est, they covered the entire basin, were probably in excess of 80 m deep and were chemically stratified. When shallow they were often playas, sometimes saline, and frequently dry, with a hard cracked surface or a cover of vegetation.

Systematic variations in successive Van Houten cycles from the deepest to shallowest lakes trace out a hierarchy of larger cycles (figure 3). There are cycles comprising an average of 5 Van Houten cycles, called short modulating cycles; cycles made up of roughly 4 short modulating cycles, called McLaughlin cycles; and cycles comprising roughly 4.4 McLaughlin cycles, called long modulating cycles (Olsen *et al.* 1996*a*). Detailed Fourier and time-frequency analysis of the Newark Basin cores shows that this hierarchy of cycles is present through the entire post-Stockton section. A measure of lake depth based on sedimentary structures, or depth rank, has been the proxy of climate used for the numerical analysis (figure 2) (for details see Olsen & Kent 1996). Based on calibration in time by palaeontological correlation to available radiometric dates, as well the structure of the Fourier spectra themselves, the cycles correspond very closely in time to the predictions of precession-related orbital forcing (Olsen & Kent 1996).

Palaeomagnetic analysis of the cores and outcrops demonstrated that individual

Van Houten cycles and the longer cycles they comprise can be correlated with confidence over tens to hundreds of kilometres (Kent *et al.* 1995; Olsen *et al.* 1996a). The lake level cycles thus represent basin-wide events. The palaeomagnetic data also show that the location of the Newark Basin drifted from about the Equator to *ca.* 10° N during the Late Triassic. Hence the lakes that produced the Newark Basin cyclicity were tropical and the control on lake depth was most likely by precipitation variations governed by the migration of the zone of tropical convergence under the control of insolation variations. The rather strong expression of the cyclicity and the implied strong links to celestial mechanics may reflect the extreme land–sea contrast caused by an equatorially centred Pangean supercontinent (Kutzbach & Gallimore 1988; Kutzbach 1994; Crowley *et al.* 1992).

(b) Stockton formation cycles

The Stockton Formation has generally been regarded as fluvial, and, therefore, in previous papers we have omitted the formation from cyclostratigraphic analysis (e.g. Olsen & Kent 1996). However, Turner-Peterson & Smoot (1985) argued that at least part of the Stockton was fluvio-deltaic and lacustrine. Further, Reynolds (1993) showed that the Upper Stockton, sandy in outcrop, became seismically indistinguishable from the Lockatong at depth, consistent with Turner-Peterson & Smoot (1985). Finally, Kent & Olsen (1997) working in the Triassic Dan River Rift Basin of North Carolina found that strata correlative with the Upper Stockton (based on palaeomagnetics) was composed of strongly cyclical lacustrine strata, at least part of which was sandy and closely comparable with the Upper Stockton in facies. This led to a reconsideration of the Upper Stockton Formation, particularly the Raven Rock Member, in the Newark cores (Kent & Olsen 1999a), and their interpretation as predominately lacustrine and deltaic, rather than strictly fluvial. Therefore, we have incorporated colour data from the core record in our analysis of Newark Basin cyclicity (figure 2) and recognize eight cycles comparable with McLaughlin cycles within the Raven Rock Member.

2. Newark Basin record tuned to the 400 ka cycle

There is now, we believe, ample evidence that precession-related forcing of lake depth is recorded in detail in the Newark Basin cores and not surprisingly is close to the pattern seen in present celestial mechanics. However, the real value of the climate time-series represented by these cores certainly rests in the application of the record to understanding what cannot be gained by looking at the present. We use the Newark Basin record as the basis for an astronomically tuned time-scale for the Late Triassic and use of the great length of the record for understanding of the role of very long-period climate cycles, which, although predicted by celestial mechanics, have rarely been observed (e.g. Lourens & Hilgen 1997).

The first step is tuning the time-series of proxies of lake depth, and hence climate, to a uniform time-scale. To do this we use a pure 404 ka cycle as the target time-series, and the depth rank and the rock colour depth series as the climate proxies (figure 4). The original depth rank and colour time-series are given in Olsen & Kent (1996) and Olsen *et al.* (1996a) and are not repeated here. The 404 ka cycle was used here because the sediment cycle (the McLaughlin cycle) produced by this climate

cycle is very obvious and it is the least likely of any of the astronomical cycles to change due to chaos in the behaviour of the Solar System over hundreds of millions of years (Laskar 1990). Only the pre-basalt portion of the Newark Basin was used for this analysis. Omission of the Jurassic syn- and post-extrusion section only removes *ca.* 1 Ma (3%) of data from consideration, however.

For the target time-series we use a value of 404 ka for the period of the '400 ka' cycle, which is based on the values for the secular frequencies of the Solar System presented by Laskar (1990) and the insolation time-series of Berger & Loutre (1991). A target 5049 m depth series was constructed with a sine wave of 65.55 m period with a sampling interval of 1.16 m. The value of 65.55 m corresponds to the thickness of the McLaughlin cycle in the upper part of the Rutgers core, which was the reference section to which all the other cores were calibrated for the composite section (Olsen *et al.* 1996*a*) (figure 4). We assume that the 65.55 m average McLaughlin cycle was caused by the 404 ka astronomical cycle. We smoothed depth series of colour and depth ranks, designed to highlight the McLaughlin cycles (figure 4), by using a moving average with a triangular window with a half-length of 27.4 m. As an alternative, we also filtered the two depth series with a zero-phase bandpass filter of 0.002 13 and 0.002 44 cycles per metre. The depth values for the peaks of smoothed and filtered depth series were virtually identical and were averaged to use as tie points to the peaks in the target 404 ka times series (figure 4). The inverse correlation technique of Martinson *et al.* (1987) as implemented in the program AnalySeries for the Macintosh™ (Paillard *et al.* 1996) was used to tune the depth records to the 404 ka time-series using the tie points described above and a cubic-spline interpolation method. The depth rank and colour depth series were tuned independently but resulted in identical depth scales. The depth scales of the tuned depth series were converted to time using a sedimentation rate of 65.55 m/404 ka. The top of the time-series was fixed at 202 Ma BP, based on radiometric dates from the overlying basalts (see Kent & Olsen 1999*a*). The age depth relationship is shown in figure 5, and the resulting time-series of depth ranks and rock colour are shown in figure 6. The sedimentation rate time-series derived from the tuning procedure is shown in figure 7 along with the tuned smoothed filtered time-series. Tuning was not performed below the Raven Rock Member of the Stockton data. Rather, the average accumulation rate for the Raven Rock Member was extrapolated through the rest of the formation. The time-series of colour and depth rank provide the basis for a time-scale for the Late Triassic, as well as an analysis of the low-frequency cycles in the Newark record as developed below.

3. Time-frequency analysis

Evolutive joint space–frequency analysis (or spectrogram analysis) was performed on the original depth rank series by Olsen & Kent (1996) to examine the persistence of the Milankovitch properties through the Newark core record, without requiring selection of sedimentation rates. Now with the depth series tuned to the 404 ka cycle it becomes possible to look at the data using true time-frequency analysis (figure 6). For this analysis, the LabView™ Joint Time-Frequency Module for the Macintosh™ was used with a sampling lag of 940 ka and 200 point Hanning window. From the spectrograms (figure 6), some of the basic Milankovitch properties can be seen through all of the Raven Rock and younger portions of the cores. Specifically,

P. E. Olsen and D. V. Kent
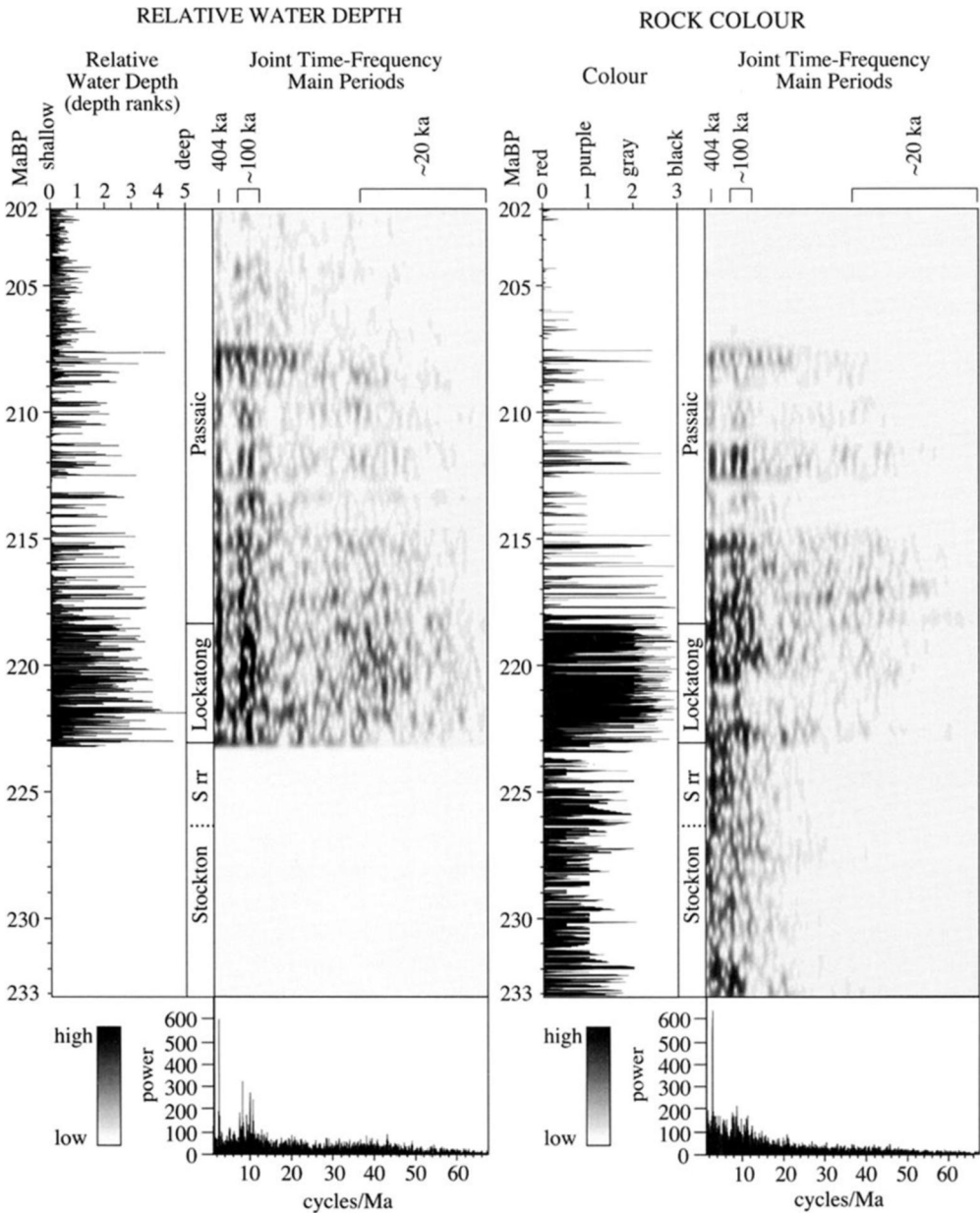
Figure 6. Joint time-frequency spectrograms of the Newark cores. Tuned depth rank and colour series are shown along with the bulk power spectrum (FFT). Srr represents the Raven Rock Member of the Stockton Formation and the label Stockton, applies to the rest of the formation.

the two peaks in power centred around 100 ka can be seen in both the colour and depth rank time-series, particularly in the latter. However, the colour spectrogram does not resolve as clearly the split *ca.* 100 ka in the Lockatong Formation, because it is mostly grey and black, reducing the range of the colour by one-third. This colour change has no effect on the depth ranking, so the tuning process resolved the

100 ka cycle clearly over the same interval. Power in the range of climatic precession (*ca.* 20 ka) is washed out due to the large dynamic range of the variance and also clear sedimentation rate changes in the same time range as the Van Houten cycles (i.e. frequency modulation (see Olsen & Kent 1996)). The climatic precession cycles were fully documented, however, by Olsen & Kent (1996) using standard Fourier methods and will not be repeated here.

A low-frequency pulsation of spectral power can be seen in the spectrograms, which appears somewhat different in the two time-series (figure 6). This occurs at what appear to be *ca.* 2 and 3–5 Ma intervals, the former corresponding to the long modulating lithological cycle. A cycle thought to be close to 1.8 Ma was observed prior to tuning and was ascribed to the *ca.* 2 Ma cycle of modulation of climatic precession by 'eccentricity' by Olsen & Kent (1996) and was in fact postulated on the basis of outcrop studies even before the cores were collected (Olsen 1986). Smoothed and filtered depth rank and colour time-series show the same basic pattern of low-frequency modulation. With a tuned time-series in depth rank and colour, these low-frequency cycles can now be examined in the frequency domain using spectral analysis.

4. Multitaper spectral analysis

We used multitaper spectral analysis (Thomson 1982; Yiou *et al.* 1994) in the Analy-Series program to examine the low-frequency cycles in the depth rank, colour, and climatic precession time-series (figure 8). For all we used a sampling interval of 2.17 ka, bandwidth-to-window product of 4, and six windows. For precession we used the positive portion of the 10 Ma series of Laskar (1990), clipped at zero so that the low-frequency cycles could be examined and compared with the depth rank and colour results.

As described in detail in previous publications (e.g. Olsen *et al.* 1996*a*), Newark core record shows virtually no indication of the *ca.* 40 ka inclination cycle. This is to be expected by relatively local astronomical forcing in the tropics (Short *et al.* 1991). The absence of a *ca.* 40 ka frequency cycle in the data makes it much less likely that the long-period modulators of inclination will be a major part of the signal, although teleconnections are obviously possible (see below). In contrast, the *ca.* 20 ka cycles of climatic precession are very strong, as are the *ca.* 100 ka and 404 ka modulating cycles of precession (i.e. eccentricity cycles). Hence, the longer-period modulators of climatic precession should be present as well, given the length of the record. For these reasons we identify the major periodic components of the spectral analysis of the tuned record as primarily long-period eccentricity cycles and identify them specifically by their proximity in frequency to predicted cycles in the Laskar90 solution (see figure 9) (tables 1 and 2).

The results of the spectral analysis show highly significant periods at the expected *ca.* 100 ka range, in fact with the *ca.* 97 and *ca.* 128 ka regions clearly resolved in all spectra (figures 8 and 9; table 2). In the precession time-series the expected 2.3 Ma, 962 ka, and 697 ka peaks are well-defined (figure 8) and significant. Highly significant, low-frequency peaks with periods averaging 1.753 Ma, 1.012 Ma and 728 ka are present in the depth rank and colour time-series, and we hypothesize that these correspond to the low-frequency cycles seen in the precession series. Visual inspection reveals that the *ca.* 1.75 Ma cycle is the low-frequency modulator of depth ranks seen

Table 1. *Origin of present values of eccentricity cycles based on the fundamental frequencies of the planets*

(The combinations of the fundamental frequencies that produce the periods of the predicted eccentricity cycles are listed in order of their amplitudes according to Laskar (1990).)

planet or name of cycle	fundamental frequency	present freq. ($''$ a^{-1})	present freq. (cycles a^{-1})	present periods (years)
Mercury	g_1	5.596	4.318×10^{-6}	231 600
Venus	g_2	7.456	5.753×10^{-6}	173 800
Earth	g_3	17.365	1.340×10^{-5}	74 630
Mars	g_4	17.916	1.382×10^{-5}	72 340
Jupiter	g_5	4.249	3.278×10^{-6}	305 000
Earth	s_3	-18.851	-1.455×10^{-5}	68 750
Mars	s_4	-17.748	-1.369×10^{-5}	73 020
—	$g_4 + s_4 - s_3 = g_{19}$	16.813	1.297×10^{-5}	77 090
E 404 ka	$g_2 - g_5$	3.207	2.475×10^{-6}	404 100
E 2.4 Ma	$g_4 - g_3$	0.551	4.250×10^{-7}	2 352 900
E 962 ka	$g_1 - g_5$	1.348	1.040×10^{-6}	961 700
E 697 ka	$g_2 - g_1$	1.860	1.435×10^{-6}	697 000
E 95 ka	$g_4 - g_5$	13.667	1.055×10^{-5}	94 800
E 124 ka	$g_4 - g_2$	10.460	8.071×10^{-6}	123 900
E 99 ka	$g_3 - g_5$	13.116	1.012×10^{-5}	98 800
E 131 ka	$g_3 - g_2$	9.909	7.646×10^{-6}	130 800
E 105 ka	$g_4 - g_1$	12.319	9.505×10^{-6}	105 200
E 139 ka	$g_{19} - g_2$	9.357	7.220×10^{-6}	138 500
E 99 ka	average	13.036	1.006×10^{-5}	99 400
E 131 ka	average	9.909	7.646×10^{-6}	131 100
E 115 ka	average	11.064	8.674×10^{-6}	115 300

in figures 2, 6 and 7. In addition, a 3.5 Ma cycle is present that does not correspond to anything in the modulation of climatic precession, but could be a long-period modulation cycle of obliquity. If so it must come from indirect forcing (telecommunications).

We also conducted multitaper spectral analysis on the sedimentation rate timeseries derived from tuning the depth rank and colour depth series (figure 9). We feel it is of considerable importance that significant cycles with a concentration of power occur at 1.742 Ma and 990 ka, very close to the 1.753 Ma and 1.012 Ma cycles present in the depth rank series. There is a concentration of coherence around these periods as well (figure 9). This shows that the sedimentation rate varies as a function of the lake water depth, and very strongly shows that at least the *ca.* 1.75 Ma cycle is a very important part of the forcing of lake record.

We are not completely alone in suggesting the potential importance of long-period cycles. Matthews & Frohlich (1991) suggested that the long-period (*ca.* 2 Ma) modulation of climatic precession should have climatic consequences and attempted to explain long term modulation of the Antarctic Ice Sheet with this cycle. In addition,

Table 2. *Present and observed Newark periods of major eccentricity cycles*

(A, Origin from fundamental; B, present frequency ($''$ a^{-1}); C, calculated (from figure 8) MTM periods Laskar90 (years); D, Newark periods (from figure 8) colour (years); E, Newark periods (from figure 8) depth rank (years); F, Newark periods (from figure 9) sedimentation rate periods (years); G, average observed Newark periods (years). (Average in column G includes only depth rank and colour periods. With the sedimentation rate periods included the averages for E 2.4 Ma and E 962 ka with average periods become 1 749 000 years and 1 004 000 years.))

name	A	B	C	D	E	F	G
E 404 ka	$g_2 - g_5$	404 100	408 000	—	—	—	—
E 2.4 Ma	$g_4 - g_3$	2 352 900	2 342 000	1 740 000	1 766 000	1 742 000	1 753 000
E 962 ka	$g_1 - g_5$	961 700	999 000	918 000	1 105 000	990 000	1 012 000
E 697 ka	$g_2 - g_1$	697 000	672 000	715 000	740 000	—	728 000
E 99 ka	average	99 400	97 000	94 000	98 000	—	96 000
E 131 ka	average	131 100	127 500	126 000	129 000	—	127 500
E 115 ka	average	115 300	112 300	110 000	113 500	—	111 800

Hilgen *et al.* (1995) noted the presence of a *ca.* 2 Ma year cycle in their Neogene records, as did Lourens & Hilgen (1997). We suspect that as very long records of orbital forcing become available that these long-period cycles will be more commonly recognized.

(a) *Possible hiatuses as a cause of the 1.75 Ma cycle*

An alternative interpretation of the 1.75 Ma cycle, relevant to both the completeness of the time-scale itself, and the period of the long term cycles, is that there could be significant hiatuses in the driest phases of the long-modulating cycles. These would correspond to times of eccentricity minima. Indeed, considering the general half-graben geometry of the basin, one might expect sequence boundaries and attendant hiatuses along the flanks of the basin during prolonged times of low lake level. The omission of just one 404 ka cycle from an interval of low eccentricity would mean that the observed period of 1.75 Ma of that cycle would actually correspond to an actual value of 2.15 Ma, which is much closer to the present 2.35 Ma period of this cycle of eccentricity. The tuning procedure we have used assumes there is but one cryptic 404 ka cycle in these zones of low eccentricity and low lake level. This results in a model accumulation curve that has a peak in accumulation rate exactly over these zones (see figure 7).

We have tested this model by examining the high-frequency cycles (i.e. Van Houten cycles) in the NBCP cores through these intervals. Here we present the results of the most extreme case, member T-U in the Rutgers no. 1 core (figure 7, cycles 25–30), although the results apply to the other similar zones as well.

In both colour and depth rank, there is an interval with basically no change (red and 0 depth rank) from the middle of member T to the base of the Kilmer Member (figure 10). We have assumed in our tuning procedure that there is only one additional member (U) in this zone, thus requiring an increase in accumulation rates over that seen in the surrounding members and 404 ka cycles. However, since there is
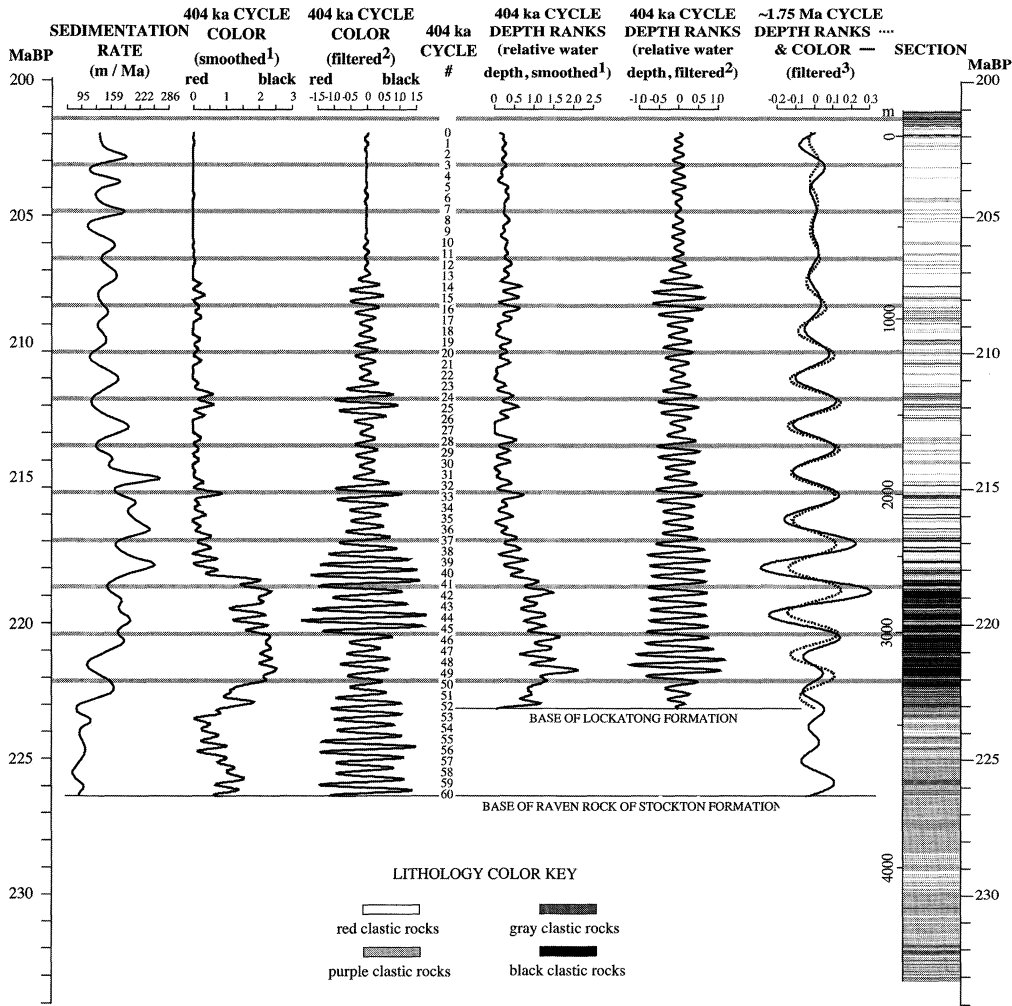
Figure 7. Tuned long cycles from the Newark cores. [1]Colour time series smoothed with a moving average with centred triangular averaging operator with 169 ka half-width to highlight 404 ka cycle. [2]Colour and depth rank time-series filtered with a zero-phase bandpass filter between the frequencies 2.48 to 0.27 cycles Ma^{-1} to highlight 404 ka cycle. [3]Colour and depth rank series filtered with a Gaussian filter at frequency 0.58 to 0.15 cycles Ma^{-1} to highlight *ca.* 1.75 Ma cycle. Grey bands are placed at 1.75 Ma intervals.

no variation in this interval in colour or depth rank, we require a different proxy of lake depth for further investigation.

Reynolds (1993) has shown that a number of geophysical logs track depth ranks very well, most notably the sonic logs. In fact, the sonic logs not only record the cycles that are recorded in depth ranks, but also show similar detail, of lower amplitude, where there is no variation in colour or depth ranks (figure 10). The dt sonic log is particularly sensitive to the Van Houten cycles. The dt sonic log is the sonic travel time divided by the interval of measurement (*ca.* 0.3m) measured in milliseconds, and is the inverse of the P-wave velocity (see Goldberg *et al.* (1994) for a full explanation).
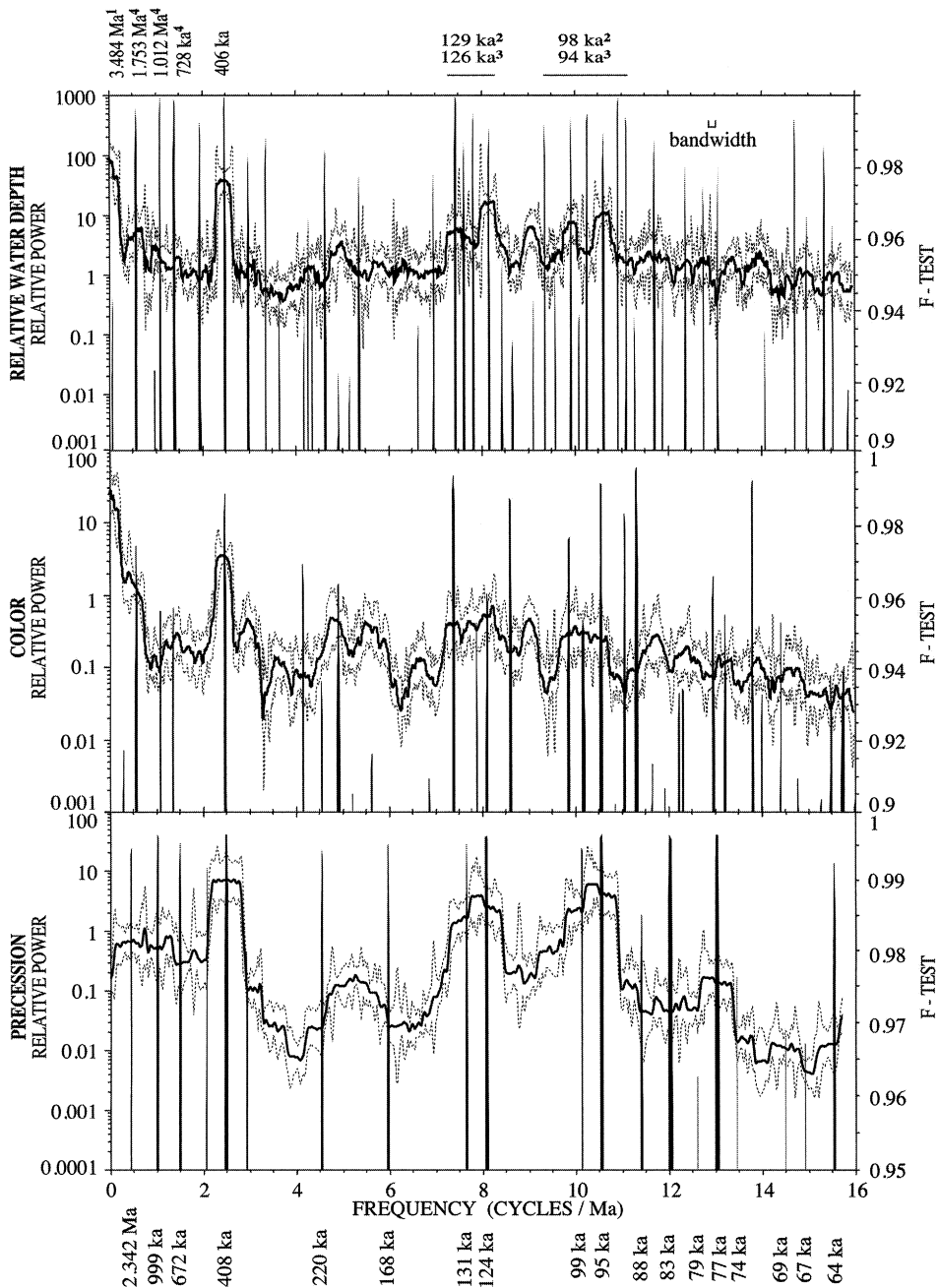
Figure 8. Multitaper method power spectra of the depth rank, colour, and clipped climatic precession time-series. Heavy line is raw power; dotted lines are upper and lower 90% confidence limits; and the black vertical spikes are the F-test statistics. Bandwidth is the same for all spectra. [1]Cycle significant only in colour time-series, but concentration of power is present at this frequency in the depth rank time-series. [2]From depth rank power spectrum. [3]From colour power spectrum. [4]Average of depth ranks and colour as follows: 1.765 Ma and 1.740 Ma; 1.105 Ma and 918 ka and 740 ka and 715 ka for depth rank and colour, respectively.
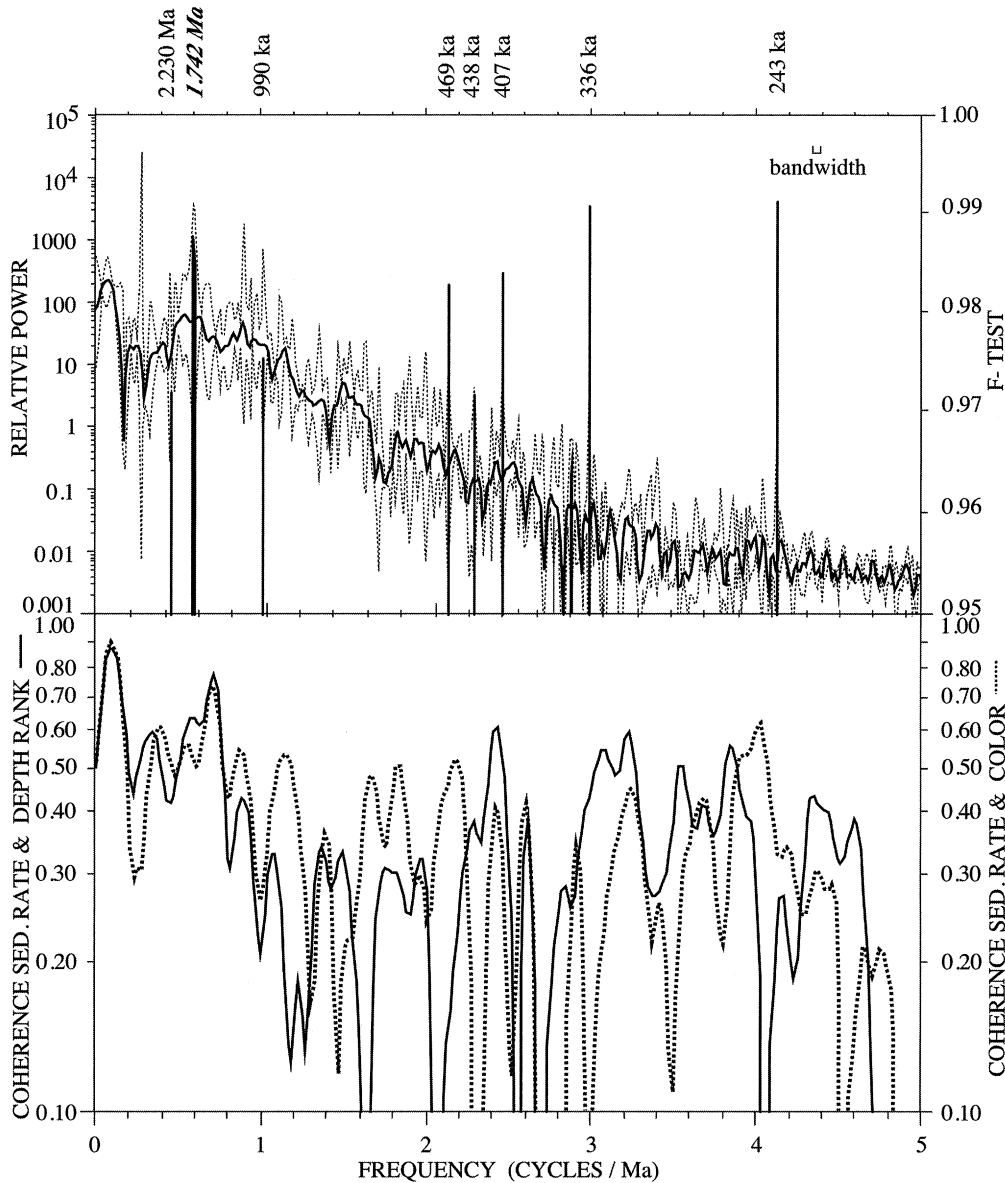
Figure 9. Multitaper method power spectrum of sedimentation rate time-series (above) derived from the tuning procedure (figures 2 and 7), compared with coherence spectra of the depth rank and colour time-series with the sedimentation rate time-series (below). Conventions for Multitaper method power spectrum are the same as in figure 8. 95% confidence level is at 0.6 in the coherency plot.

The logs are evidently tracking higher velocities in the more cemented beds, and these are associated with the deeper lakes. These variations are visible in the cores to some extent, but they do not fit into to the depth rank scheme. The correspondence to depth rank is very strong where there are depth ranks greater than zero.

We have examined this interval with evolutive joint space–frequency analysis (fig-
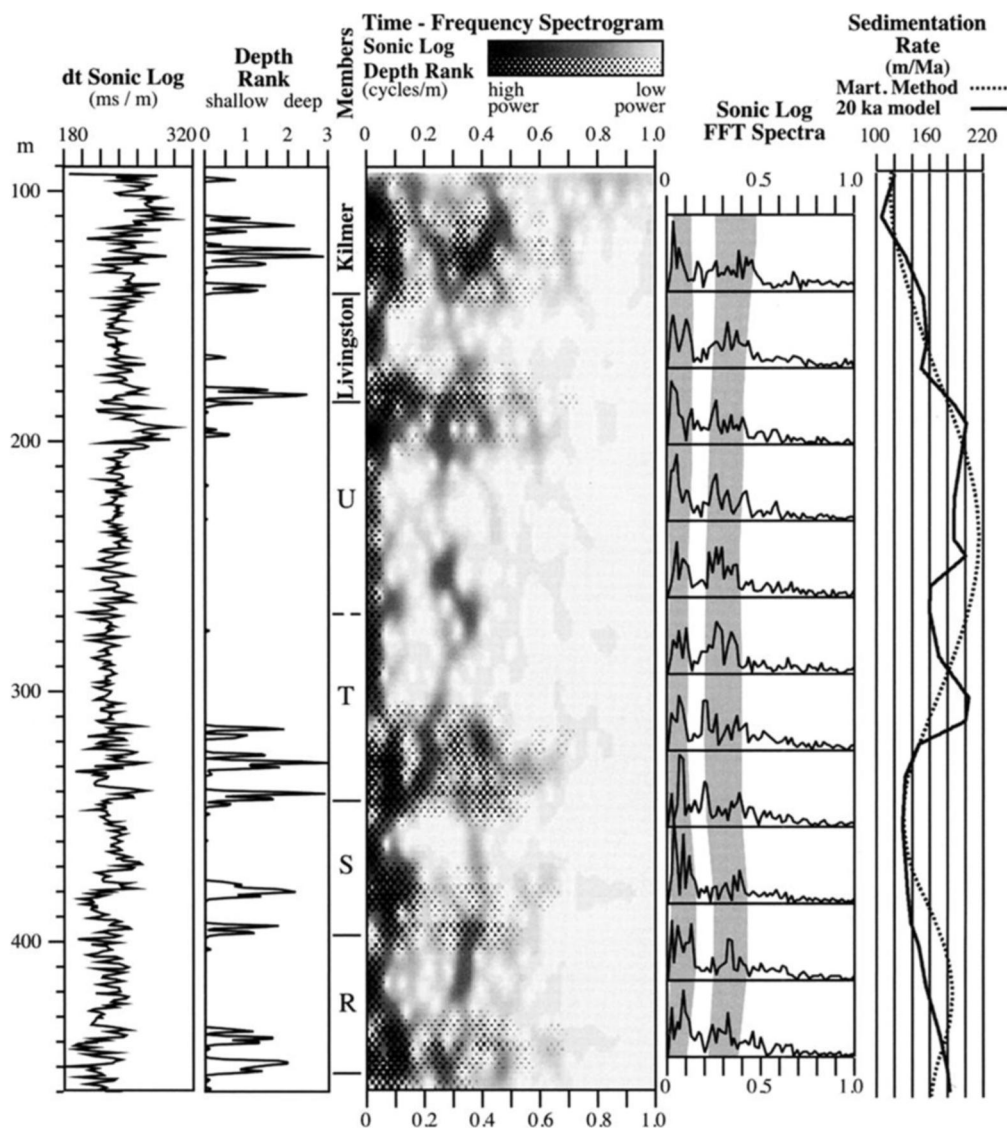
Figure 10. Evolutive analysis of high-frequency cycles in depth ranks and dt sonic logs of members R though Kilmer and evolutive spectral analysis in the Rutgers no. 1 core (depth ranks) and core hole (dt sonic log). These are raw, untuned data in hole and core depth. Spectrograms were produced using a 15 m window and a sampling rate of 0.15 m. Units of the power spectra and spectrogram are in cycles per metre.

ure 10) and a simple moving window FFT (figure 10). Both show the same hierarchical pattern of cyclicity in the dt sonic log data. The depth rank spectrogram shows concentrations of power directly overlapping that of dt sonic (figure 10). Based on both the spectrogram and the moving window FFTs, the concentration of power in the high-frequency part of the spectra shifts from relatively higher frequencies in member S to lower frequencies in T and U and then higher frequencies again up

into the Kilmer and Livingston members. This change corresponds to an accumulation rate of $ca.\ 100$–140 m Ma^{-1} in the Kilmer Member, 140–160 m Ma^{-1} in the Livingston Member, 160–200 m Ma^{-1} in member U, 120–200 m Ma^{-1} in member T, and 120–140 m Ma^{-1} in member S. This is very close to the predicted accumulation rates based tuning to the 404 ka cycle (figures 7 and 10). In addition, member U, which is not expressed in colour or depth rank, is very well defined by the dt sonic logs. Similar results were obtained in other intervals such as that adjacent to member C. We regard this as very strong independent corroboration of the tuning method and of the reality of the 1.75 Ma period of the long modulating cycle during Late Triassic time.

5. Implications for the behaviour of the inner planets

Sussman & Wisdom (1988, 1992) and Laskar (1989, 1990) have shown that when examined over long periods of time the motions of the planets are chaotic. This chaos is reflected in a slow drift in the stabilities of the fundamental frequencies of the planetary system (g_i and s_i), which means that the exact motion of the planets cannot be computed over time-scales greater than 100 Ma. The g_i and s_i frequencies are derived from Fourier analysis of a numerical integration of planetary motions, and are expressions of the moving figures of the planetary orbits, there being one g and one s for each planet (e.g. g_3 is for Earth) (Berger *et al.* 1992). The g_i frequencies reflect eccentricity, and the s_i frequencies the inclination of the orbits. These frequencies are used in the calculation of the major variations in the Earth's orbit that can influence the Earth's climate. Because of the drift in these values, it is not possible, by existing methods, to exactly calculate the classical celestial mechanical frequencies of importance to palaeoclimate and therefore astronomical tuning of very ancient geological time-scales. However, as pointed out by Berger *et al.* (1992) and Berger & Loutre (1994), the predicted size of the chaotic zones is so small that the chaos will have a negligible effect on the frequencies generally thought to be of palaeoclimatic importance. Indeed, uncertainties in the history of the recession of the Moon and water and land mass distribution on the Earth's surface are of much greater importance in calculating the high-frequency cycles. However, a major effect of the drift in g and s of the planets is seen in calculation of the longest period cycles of both eccentricity and obliquity.

The frequencies of the eccentricity cycles as they effect Earth can be calculated by linear combinations of g_i and s_i of the planets (Berger & Loutre 1990) (table 1). Based on the size of the chaotic region given by Laskar (1990), calculation of the periods of the low-frequency cycles seen in eccentricity (and in the modulation of climatic precession) shows almost no variability in the 404 ka cycle but huge possible variation in the cycles with periods greater than $ca.\ 0.5$ Ma, in some cases amounting to more than 45% deviation from the present value. The envelope of climatic precession is profoundly modulated by these long-period cycles and therefore the longer cycles should be seen in long geological records in which climatic precession is reflected. This is certainly the case with the Newark Basin core record and it seems very likely to us that the longer-period cycles seen there are attributable to the modulation of precession.

We have calculated the fundamental frequencies of the inner planets by solving for g_1, g_3, and g_4 (for Mercury, Earth, and Mars) by assuming no significant variation

Table 3. *Origin of present eccentricity cycles of the inner planets*

(The values based on the observed Newark frequencies are boldface. A, Fundamental frequency; B, present frequency ($'' a^{-1}$); C, present frequency (cycles a^{-1}); D, present periods (years); E, Newark frequency ($'' a^{-1}$) (calculated on the basis of the Newark g values); F, Newark frequency (cycles a^{-1}); G, Newark periods (years).)

| planet	A	B	C	D	E	F	G
Mercury	g_1	5.596	4.318×10^{-6}	231 600	**5.530**	$\mathbf{4.267 \times 10^{-6}}$	**234 400**
Venus	g_2	7.456	5.753×10^{-6}	173 800	7.456	5.753×10^{-6}	173 800
Earth	g_3	17.365	1.340×10^{-5}	74 630	**17.220**	$\mathbf{1.329 \times 10^{-5}}$	**75 300**
Mars	g_4	17.916	1.382×10^{-5}	72 340	**17.959**	$\mathbf{1.386 \times 10^{-5}}$	**72 200**
Jupiter	g_5	4.249	3.278×10^{-6}	305 000	4.249	3.278×10^{-6}	305 000
E 404 ka	$g_2 - g_5$	3.207	2.475×10^{-6}	404 100	3.207	2.475×10^{-6}	404 100
E 2.4 Ma	$g_4 - g_3$	0.551	4.250×10^{-7}	2 352 900	0.739	5.705×10^{-7}	1 753 000
E 962 ka	$g_1 - g_5$	1.348	1.040×10^{-6}	961 700	1.218	9.881×10^{-7}	101 200
E 697 ka	$g_2 - g_1$	1.860	1.435×10^{-6}	697 000	1.780	1.374×10^{-6}	72 800
E 99 ka	average calculation	13.036	1.006×10^{-7}	99 400	13.034	1.006×10^{-7}	99 470
	average observation	—	—	—	**13.252**	$\mathbf{1.012 \times 10^{-7}}$	**96 000**
E 131 ka	average calculation	9.909	7.646×10^{-6}	131 100	9.908	7.6453×10^{-6}	129 430
	average observation	—	—	—	**10.048**	$\mathbf{7.753 \times 10^{-6}}$	**127 500**
E 115 ka	average calculation	13.036	1.006×10^{-7}	115 300	13.034	1.006×10^{-7}	114 450
	average observation	—	—	—	**13.252**	$\mathbf{1.012 \times 10^{-7}}$	**111 800**
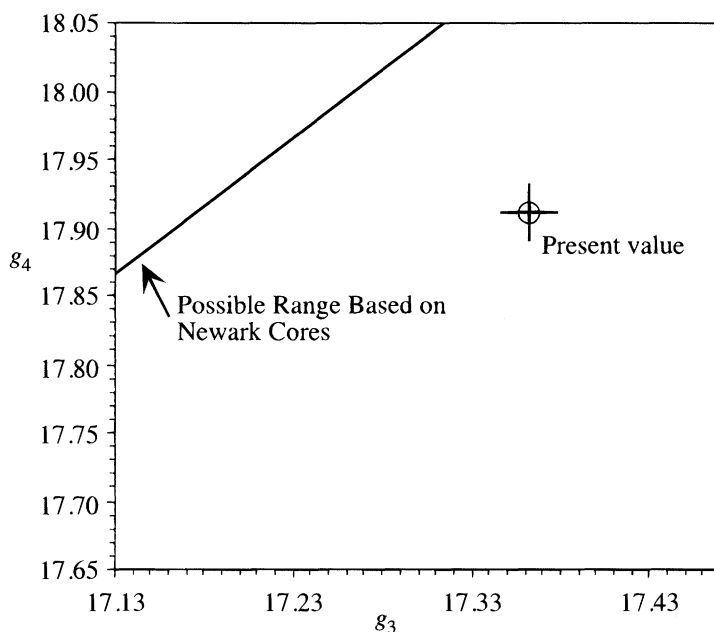
Figure 11. Range of possible g_3 and g_4 values based on the Newark cores and limited by the size of the chaotic zone as defined by Laskar (1990).

in g_5 or g_2 (Jupiter and Venus) and assuming that the 1.753 Ma, 1.012 Ma, and 728 ka cycles are those with the present day frequencies $g_4 - g_3$ (2.4 Ma), $g_1 - g_5$ (962 ka), and $g_2 - g_1$ (697 ka), respectively. Because, both g_3 (Earth) and g_4 (Mars) have rather large chaotic regions it is not possible to separate their potential mutual interactions based on the data presented here. However, the region within the chaotic zones of g_4 and g_3 can be clearly defined (table 3, figure 11). It is obvious that if any possible combination of g_4 and g_3 values within the chaotic region are equally plausible, then the values calculated based on these geological data are reasonable. We note, however, that the rate of change of g values is sufficiently large (based on Laskar 1990), especially in the case of g_4, that it may be possible to see changes in the periods of the longer cycles within the Newark record itself, a possibility not explored here. Nonetheless, for at least the Lockatong and Passaic Formation, the 1.75 Ma period appears stationary.

When the g values we calculate from the Newark records are used to predict the values of the *ca.* 100 ka cycles, we find very good agreement with the observed Newark average periods (table 1), in agreement with Berger *et al.* (1992) and Berger & Loutre (1994). We note, also, that these tuned results for the *ca.* 100 ka cycles are much cleaner than those based on the untuned data by Olsen & Kent (1996).

The geological record is the only source of information that can allow the specification of the actual g values of the past. This can be done, however, only if the geological records are of sufficient length and sensitivity to resolve the long-period cycles, as is the case in the Newark cores. In addition, there has always been a possibility that chaos in the Solar System is only a numerical artefact as pointed out by Sussman & Wisdom (1992). We feel that the Newark results, presented here, are

powerful arguments in favour of the reality of this chaos, and are a step towards its calibration.

6. Late Triassic time-scale

Combined with palaeomagnetic and biostratigraphic data, the tuned depth rank and colour time-series provide the basis for a high resolution time-scale for the Late Triassic (figure 11). The Triassic–Jurassic boundary occurs in the uppermost Passaic Formation based on pollen and spore and vertebrate biostratigraphy (Fowell & Olsen 1993; Olsen *et al.* 1987, 1990). Its age is placed at 202 Ma BP, based on ^{40}Ar/^{39}Ar and U–Pb radiometric dates from feeders to the overlying lava flows (Ratcliffe 1988; Sutter 1988; Dunning & Hodych 1990), well within the error range of the most recent compilation of the Mesozoic time-scale (Gradstein *et al.* 1994) and very close to new U–Pb dates for tuffs interbedded with marine strata (Pálfy *et al.* 1998).

Biostratigraphic data are very scarce from the basal Stockton Formation. However, the presence of the very large non-metoposaurid amphibian *Calamops paludosus* (Sinclair 1917) suggests correlation to the basal Late Triassic (Julian, Early Carnian) or Middle–Late Triassic (Carnian–Ladinian) boundary. The minimal nominal astronomical age of 233 Ma BP for the base of the Newark section, which appears to be still of Carnian age, is consistent with 238–341 Ma BP ages of Brack *et al.* (1996) for strata within the Ladinian (Kent & Olsen 1999*b*).

The Upper Stockton through Upper Passaic formations produce a very much richer array of biostratigraphically useful fossils, allowing a much stronger stage or sub-stage level correlation with strata in other areas (figure 12) (Cornet 1993; Huber & Lucas 1996; Olsen 1988).

Kent & Olsen (1999*a, b*) used the boundaries of lithostratigraphic mapped members of the Lockatong and Passaic formations and lithological cycles in the Raven Rock Member of the Stockton as a basis for converting the Newark Basin depth scale to time. This was done under the assumption that these members correspond fairly closely to McLaughlin lithological cycles and these in turn were produced by the 404 ka climatic cycle. This requires the recognition of cycle boundaries, while the presumed climatic forcing was in fact sinusoidal. Our time-scale presented here (figure 12) requires no specific typological identification of cycle boundaries and assumes only that the lithological response to the longer-period cycles was also sinusoidal. It is with considerable satisfaction that we note that the time-scale derived by both methods are nearly indistinguishable.

We incorporate the 58 complete normal and reverse polarity magnetozones described in Kent *et al.* (1995) into the time-scale as described in Kent & Olsen (1999*a, b*). Based on detailed sampling across all polarity reversals in the Passaic Formation, Kent & Olsen (1999*a*) suggest transition durations ranging from 2 to 20 ka with a mean of 7.9 ka, similar to the estimated durations of Pleistocene polarity transitions. The polarity interval lengths have a mean duration of *ca.* 0.53 Ma, no significant polarity bias, with an approximately exponential distribution. This indicates that this reversal sequence should therefore represent an accurate chronology of reversal history for the Late Triassic and provide a high-resolution tool for essentially global correlation at a level of resolution comparable with that in the Quaternary.

The very long-period cycles (greater than 500 ka) we describe in this paper are probably not very useful on their own in calibrating the geological time-scale because
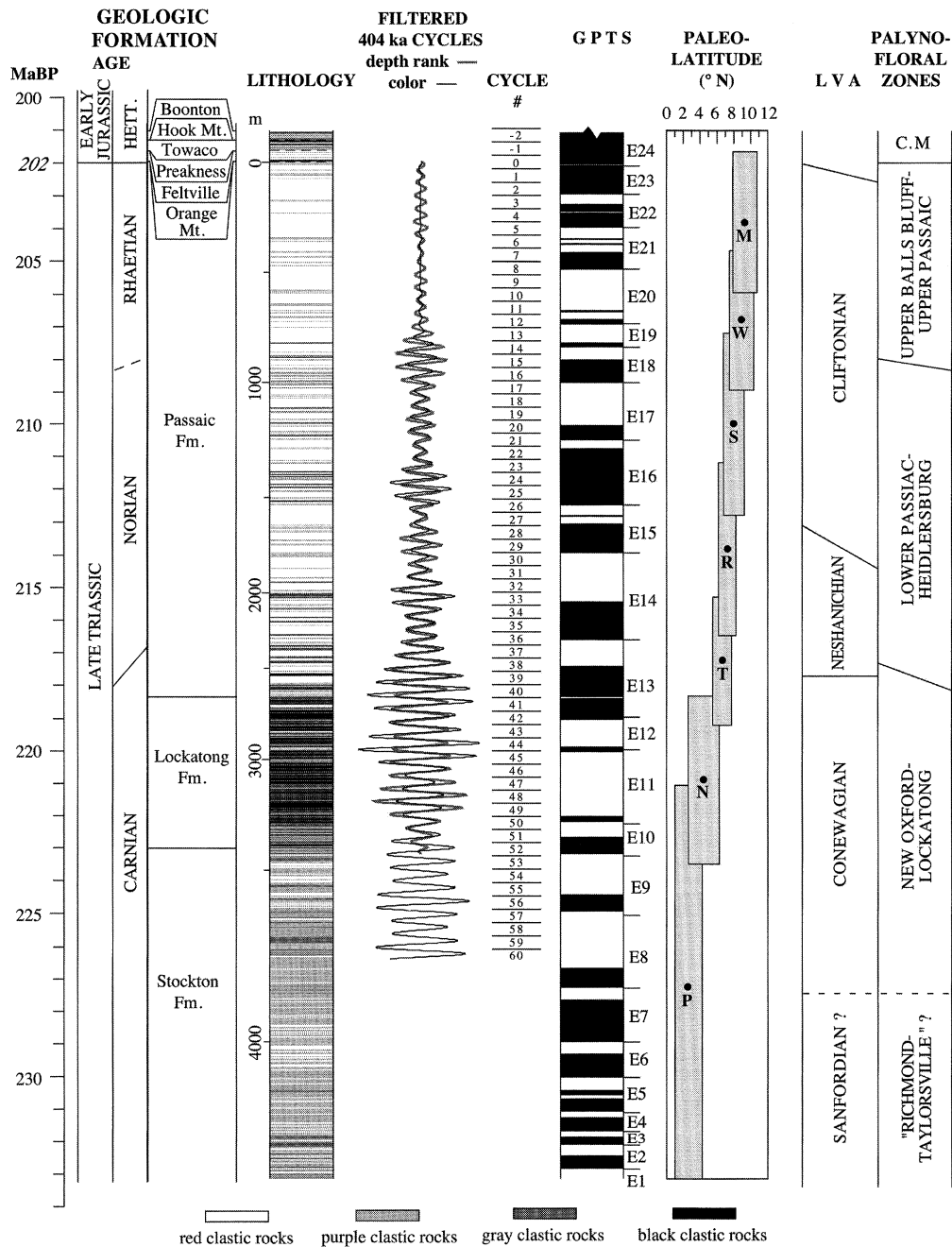
Figure 12. Time-scale for the Late Triassic based on the Newark cores. Biostratigraphic divisions from Cornet (1993) and Huber & Lucas (1996). Palaeolatitude is for the Newark Basin as it tracks north through the Late Triassic (Kent *et al.* 1995). Abbreviations are: GPTS, geomagnetic polarity time-scale (see Kent & Olsen 1999), black is normal and white is reversed polarity; LVA, land vertebrate ages (based on Huber & Lucas 1996); C.M., Corollina meyeriana palynofloral zone.

of the large uncertainties in predicted periods over several tens to hundreds of millions of years. However, the cycle due to $g_4 - g_3$ (2.4–1.8 Ma) may have great potential for geological correlation, once its period is established, especially in stratigraphic sections characterized by low average accumulation rates or many small gaps. We have already begun to use this technique in correlating across Triassic Pangea. We also note that these long cycles have the potential, through their very long 'lever arms' in establishing the very small differences between the interacting g and s values, to greatly refine the predicted periods of the higher-frequency cycles, which then can be used for high-resolution tuning of geological records.

7. Conclusions

We have tuned the Newark Basin core records of lake level changes and rock colour to the 404 ka astronomical cycle. This has allowed us to recognize and describe long-period cycles in the record that we believe are those predicted by celestial mechanics. Their values (1.75 Ma, 922 ka and 735 ka) are significantly different than present and the differences are attributable to the chaotic behaviour of the inner planets over 200 Ma. We then have used the Newark tuned record to develop a astronomically calibrated time-scale for the late Triassic that does not depend on the typological recognition of the boundaries between lithological cycles.

References

Berger, A. & Loutre, M. F. 1990 Origine des fréquences des éléments astronomiques intervenant dans le calcul de l'insolation. *Bull. Classe Sci. Acad. R. Belg.* Ser. 6 **1**(1–3), 45–106.

Berger, A. & Loutre, M. F. 1991 Insolation values for the climate of the last 10 million years. *Quat. Sci. Rev.* **10**, 297–317.

Berger, A. & Loutre, M. F. 1994 Astronomical forcing through geological time. *Int. Ass. Sediment.* (Spec. Publ.) **19**, 15–24.

Berger, A., Loutre, M. F. & Laskar, J. 1992 Stability of the astronomical frequencies over the Earth's history for paleoclimate studies. *Science* **255**, 560–566.

Brack, P., Mundil, R., Oberli, F., Meier, M. & Rieber, H. 1996 Biostratigraphic and radiometric age data question the Milankovitch characteristics of the Latemar cycles (Southern Alps, Italy). *Geology* **24**, 371–375.

Cornet, B. 1993 Applications and limitations of palynology in age, climatic, and paleoenvironmental analyses of Triassic sequences in North America. In *The nonmarine Triassic* (ed. S. G. Lucas & M. Morales), pp. 75–93. Bulletin of the New Mexico Museum of Natural History and Science, vol. 3.

Crowley, T. J., Kim, K.-Y., Mengel, J. G. & Short, D. A. 1992 Modeling the 100,000-year climate fluctuations in pre-Pleistocene time series. *Science* **255**, 705–707.

Dunning, G. R. & Hodych, J. D. 1990 U–Pb zircon and baddeleyite age for the Palisade and Gettysburg sills of northeast United States; implications for the age of the Triassic–Jurassic boundary. *Geology* **18**, 795–798.

Fedosh, M. S. & Smoot, J. P. 1988 A cored stratigraphic section through the northern Newark Basin, New Jersey. *US Geol. Surv. Circ.* **946**, 19–24.

Fowell, S. J. & Olsen, P. E. 1993 Time-calibration of Triassic/Jurassic microfloral turnover, eastern North America. *Tectonophysics* **222**, 361–369.

Goldberg, D., Reynolds, D., Williams, C., Witte, W. K., Olsen, P. E. & Kent, D. V. 1994 Well logging results from the Newark Rift Basin Coring Project. *Scientific Drilling* 4, 267–279.

Gradstein, F. M., Agterberg, F. P., Ogg, J. G., Hardenbol, J., Van Veen, P., Thierry, J. & Hauang, Z. 1994 A Mesozoic time scale. *J. Geophys. Res.* **99**, 24 051–24 074.

Hilgen, F. J., Krijgsman, W., Langereis, C. G., Lourens, L. J., Santarelli, A. & Zachariasse, W. J. 1995 Extending the astronomical (polarity) time scale into the Miocene. *Earth Planet. Sci. Lett.* **136**, 495–510.

Huber, P. & Lucas, S. 1996 Vertebrate biochronology of the Newark Supergroup, eastern North America. In *The continental Jurassic* (ed. M. Morales), pp. 179–186. Museum of Northern Arizona Bulletin, vol. 60.

Kent, D. V. & Olsen, P. E. 1997 Magnetostratigraphy and paleopoles from the Late Triassic Dan River–Danville Basin: interbasin correlation of continental sediments and a test of the tectonic coherence of Newark rift basins in eastern North America. *Geol. Soc. Am. Bull.* **109**, 366–377.

Kent, D. V. & Olsen, P. E. 1999*a* Astronomically tuned geomagnetic polarity time scale for the Late Triassic. *J. Geophys. Res.* **104**, 12 831–12 841.

Kent, D.V. & Olsen, P. E. 1999*b* Implication of astronomical climate cycles to the chronology of the Late Triassic. In *The epicontinental Triassic* (ed. G. Bachmann). Springer.

Kent, D. V., Olsen, P. E. & Witte, W. K. 1995 Late Triassic–earliest Jurassic geomagnetic polarity sequence and paleolatitudes from drill cores in the Newark rift basin, eastern North America. *J. Geophys. Res.* **100**, 14 965–14 998.

Kutzbach, J. E. 1994 Idealized Pangean climates; sensitivity to orbital change. In *Pangea; paleoclimate, tectonics, and sedimentation during accretion, zenith and breakup of a supercontinent* (ed. G. D. Klein), pp. 41–55. *Geol. Soc. Am.* Spec. Paper 288.

Kutzbach, J. E. & Gallimore, R. G. 1988 Pangaean climates: megamosoons of the megacontinent. *J. Geophys. Res.* **94**, 3341–3358.

Laskar, J. 1989 A numerical experiment on the chaotic behaviour of the Solar System. *Nature* **338**, 237–238.

Laskar, J. 1990 The chaotic motion of the Solar System: a numerical estimate of the size of the chaotic zones. *Icarus* **88**, 266–291.

Lourens, L. J. & Hilgen, F. J. 1997 Long-periodic variation in the Earth's obliquity and their relation to third-order eustatic cycles and Late Neogene glaciations. *Quat. Int.* **40**, 43–52.

McLaughlin, D. B. 1946 Continuity of strata in the Newark Series. *Mich. Acad. Sci. Arts Lett.* **32**, 295–303.

Malinconico, M. L. 1997 Contrasting thermal histories of the early Mesozoic Newark and Taylorsville Basins based on borehole and surface vitrinite reflectance; basin-wide conductive vs. advective effects. *Am. Ass. Petrol. Geol. Bull.* **81**, 1778.

Manspeizer, W. 1988 Triassic–Jurassic rifting and opening of the Atlantic: an overview. In *Triassic–Jurassic rifting and the opening of the Atlantic Ocean* (ed. W. Manspeizer), pt. A, pp. 41–79. Elsevier.

Martinson, D. G., Pisias, N. G., Hays, J. D., Imbrie, J., Moore, T. C. & Shackleton, N. J. 1987 Age dating and the orbital theory of the ice ages: development of a high-resolution 0–300,000 year chronostratigraphy. *Quat. Res.* **27**, 1–30.

Matthews, R. K. & Frohlich, C. 1991 Orbital forcing of low-frequency glacioeustasy. *J. Geophys. Res.* **96**, 6797–6703.

Olsen, P. E. 1986 A 40-million-year lake record of early Mesozoic climatic forcing. *Science* **234**, 842–848.

Olsen, P. E. 1988 Paleoecology and paleoenvironments of the continental early Mesozoic Newark Supergroup of Eastern North America. In *Triassic–Jurassic rifting and the opening of the Atlantic Ocean* (ed. W. Manspeizer), pt. A, pp. 185–230. Elsevier.

Olsen, P. E. 1997 Stratigraphic record of the early Mesozoic breakup of Pangea in the Laurasia-Gondwana rift system. *A. Rev. Earth Planet. Sci.* **25**, 337–401.

Olsen, P. E. & Kent, D. V. 1990 Continental Coring of the Newark Rift. *Eos* **71**, 385, 394.

Olsen, P. E. & Kent, D. V. 1996 Milankovitch climate forcing in the tropics of Pangea during the Late Triassic. *Paleogeol. Paleoclim. Paleoecol.* **122**, 1–26.

Olsen, P. E., Shubin, N. H. & Anders, P. E. 1987 New Early Jurassic tetrapod assemblages constrain Triassic–Jurassic tetrapod extinction event. *Science* **237**, 1025–1029.

Olsen, P. E., Fowell, S. J. & Cornet, B. 1990 The Triassic–Jurassic boundary in continental rocks of eastern North America: a progress report. In *Global catastrophes in Earth history; an interdisciplinary conference on impacts, volcanism, and mass mortality* (ed. V. L. Sharpton & P. D. Ward), pp. 585–593. Geological Society of America Special Paper 247.

Olsen, P. E., Kent, D V., Cornet, B., Witte, W. K. & Schlische, R. W. 1996*a* High-resolution stratigraphy of the Newark rift basin (Early Mesozoic, Eastern North America). *Geol. Soc. Am.* **108**, 40–77.

Olsen, P. E., Schlische, R. W. & Fedosh, M. S. 1996*b* 580 ka duration of the Early Jurassic flood basalt event in eastern North America estimated using Milankovitch cyclostratigraphy. In *The continental Jurassic* (ed. M. Morales), pp. 11–22. Museum of Northern Arizona Bulletin, vol. 60.

Paillard, D., Labeyrie, L. & Yiou, P. 1996 Macintosh program performs time-series analysis. *Eos* **77**, 379.

Pálfy, J., Smith, P. L. & Mortenson, J. K. 1998 A revised numeric time scale for the Jurassic. In *Proc. 5th Int. Symp. on the Jurassic System (Vancouver, BC, August 1998)* (ed. R. L. Hall, P. L. Smith & T. P. Poulton). Zurich: Transtec.

Ratcliffe, N. M. 1988 Reinterpretation of the relationships of the western extension of the Palisades sill to the lava flows at New York based on new core data. *US Geol. Surv. Bull.* **1776**, 113–135.

Reynolds, D. J. 1993 Sedimentary basin evolution: tectonic and climatic interaction. PhD thesis, Columbia University, New York.

Short, D. A., Mengel, J. G., Crowley, T. J., Hyde, W. T. & North, G. R. 1991 Filtering of Milankovitch cycles by Earth's geography. *Quat. Res.* **35**, 157–173.

Sinclair, W. J. 1917 A new labyrinthodont from the Triassic of Pennsylvania [*Calamops paludosus*]. *Am. J. Sci.* **43**, 319–321.

Smoot, J. P. & Olsen, P. E. 1994 Climatic cycles as sedimentary controls of rift basin lacustrine deposits in the early Mesozoic Newark Basin based on continuous core In *Lacustrine depositional systems* (ed. T. Lomando & M. Harris), pp. 201–237. SEPM Core Workshop Notes, 19.

Sussman, G. J. & Wisdom, J. 1988 Numerical evidence that the motion of Pluto is chaotic. *Science* **241**, 433–437.

Sussman, G. J. & Wisdom, J. 1992 Chaotic evolution of the Solar System. *Science* **257**, 56–62.

Steckler, M. S., Omar, G. I., Karner, G. D. & Kohn, B. P. 1993 Pattern of hydrothermal circulation within the Newark Basin from fission-track analysis. *Geology* **21**, 735–738

Sutter, J. F. 1988 Innovative approaches to dating igneous events in the early Mesozoic basins, eastern North America. *US Geol. Surv. Bull.* **1776**, 194–200

Thomson, D. J. 1982 Spectrum estimation and harmonic analysis. *IEEE Proc.* **70**, 1055–1096.

Turner-Peterson, C. E. & Smoot, J. P. 1985 New thoughts on facies relationships in the Triassic Stockton and Lockatong formations, Pennsylvania and New Jersey. In *Proc. Second US Geological Survey Workshop on the Early Mesozoic Basins of the Eastern United States* (ed. G. R. Robinson Jr & A. J. Froelich). *US Geol. Surv. Circ.* **946**, 10–17.

Van Houten, F. B. 1969 Late Triassic Newark Group, north-central New Jersey and adjacent Pennsylvania and New York. In *Geology of selected areas in New Jersey and eastern Pennsylvania and guidebook of excursions, New Brunswick, New Jersey* (Geological Society of America, Field Trip 4) (ed. S. Subitzki), pp. 314–347. New Brunswick: Rutgers University Press.

Van Houten, F. B. 1977 Triassic–Liassic deposits of Morocco and eastern North America; comparison. *Am. Ass. Petrol. Geol. Bull.* **61**, 79–99.

Witte, W. K., Kent, D. V. & Olsen, P. E. 1991 Magnetostratigraphy and paleomagnetic poles from Late Triassic–earliest Jurassic strata of the Newark Basin. *Geol. Soc. Am. Bull.* **103**, 1648–1662.

Yiou, P., Ghil, M., Jouzel, J., Paillard, D. & Vautard, R. 1994 Nonlinear variability of the climatic system, from singular and power spectra of Late Quaternary records. *Climate Dynamics* **9**, 371–389.